

d Bands in Cubic Lattices. II

JOSEPH CALLAWAY

Division of Physical Sciences, University of California, Riverside, California

(Received June 2, 1960)

The results of a previous, perturbation theoretic treatment of *d* bands in the body-centered cubic lattice are extended in several respects: The methods of the previous calculation are applied to determine energy levels at the points Γ and X in the Brillouin zone of the face-centered cubic lattice. As before, the crystal potential is that of a lattice of point charges, screened by a uniform distribution of electrons. The perturbation expansion of the wave function of a *d* electron is developed for the body-centered cubic lattice. Calculations are reported for two states near the top and bottom of the *d* band, including terms of first order in the potential. These functions have the characteristic property that the wave function of a state near the top of the *d* band is more compact than that belonging to a state near the bottom. The energies

of four states for the body-centered lattice are computed as a function of the binding parameter Za by a more accurate method than that employed in the previous work, making possible an estimation of the accuracy of perturbation theory and the dependence of bandwidth on binding parameter. The role of crystal field effects in the tight-binding limit is discussed, and the circumstances are determined under which the *d* band may split into sub-bands based on functions of different cubic symmetries. Estimation of the value of the binding parameter for which such separation occurs strongly suggests that this split does not occur for the actual transition metals. Finally, the effects of spin-orbit coupling on the band structure are studied in the tight-binding approximation. A formulation of $\mathbf{k} \cdot \mathbf{p}$ perturbation theory for *d* bands is given.

I. INTRODUCTION

IT is the purpose of the work reported on this paper to continue the general study of *d* bands in cubic lattices. A beginning was made in a previous calculation (afterwards referred to as I) in which perturbation theory with symmetrized linear combinations of plane waves as basis functions was used to study *d* bands in the body-centered cubic lattice.¹ A simple crystal model was employed which consisted of a lattice of point charges (atomic number Z , lattice parameter a) screened by a uniform distribution of negative charge.

The study of a simple model as an approach to an understanding of some features of the electronic structure of the transition metals was undertaken for the following reasons: First, the complexities of a self-consistent energy band calculation for a multivalent element with *d* electrons on the basis of the Hartree-Fock equations are so great that considerable further progress in the techniques of band calculation is probably required before quantitative results can be expected. Second, even if such a self-consistent calculation could be made for some particular metal, it might not yield much qualitative information with respect to the dependence of band structure on lattice symmetry and the relevant parameters of atomic spacing and atomic number. Such information is required for a real understanding of the properties of these metals and their alloys. Third, at various times, greatly different theories of the electronic structure of the transition metals have been proposed, some without any support in band theory, in an attempt to interpret experimental observations of their properties. This study should at least be of assistance in determining the circumstances in which more detailed theories may be expected to apply.

Of course, many features of the electronic structure of real crystals have to be neglected in our considera-

tions. Probably the most serious omission is the neglect of spin-dependent (exchange) interactions between the *d* electrons. It is hoped that the gain in simplicity and in qualitative understanding will compensate to some extent for the necessary discard of some of the complications of reality.

The principal object of this paper is to determine insofar as possible, the qualitative behavior of the *d*-band structure as one passes, continuously, from the case of free electrons to that of tightly bound electrons. Principal emphasis is placed on the body-centered cubic lattice (since there are two points in the Brillouin zone which have full cubic symmetry), but a beginning is made in the study of another structure, the face-centered cubic lattice. The wave functions of *d* electrons are briefly investigated, and some consideration is given to the effects of spin-orbit coupling.

The perturbation analysis of I may be applied to states in any structure, provided only that the symmetry of the state is such that low-energy *s* and *p* functions are not incorporated in the wave function. In Sec. II, the face-centered cubic lattice is considered. Results are given for five states at the symmetry points Γ and X (see Fig. 1). Unfortunately, the point X does not possess the full cubic symmetry of the corner H in the Brillouin zone of the body-centered cubic lattice. Consequently, one of the states of the *d* band at X (X_1)² contains *s* functions as well, so that its energy cannot be found by this method for interesting values of the relevant parameters.

In view of recent discussions of the wave functions of *d* electrons in metals (with particular attention to iron),³ it is interesting to apply the perturbation methods to a calculation of wave functions as well as energies. This is done in Sec. III for two states pertaining to the body-centered cubic lattice: H_{12} , which is

¹ J. Callaway, Phys. Rev. **115**, 346 (1959).

² Notation according to L. P. Bouckaert, R. Smoluchowski, and E. P. Wigner, Phys. Rev. **50**, 58 (1936).

³ J. H. Wood, Phys. Rev. **117**, 714 (1960).

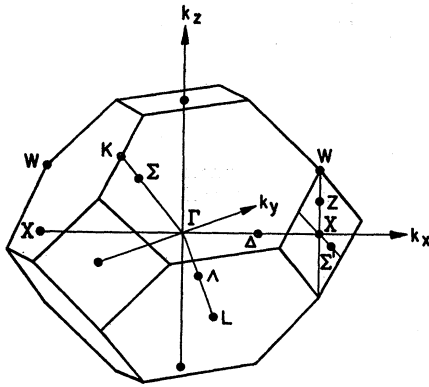


FIG. 1. Brillouin zone for the face-centered cubic lattice. Points and lines of symmetry are indicated.

close to the bottom of a normal d band, and $H_{25'}$, which is near the top. The perturbation series is in fact a Fourier series for a set of correction functions which are added to the basic plane wave function with coefficients proportional to appropriate powers of the binding parameter Za . The d part of the first such correction function (corresponding to first-order perturbation theory) is evaluated numerically for the two states considered. The result reported by Wood,³ that states at the bottom of the d band have smoother wave functions than those at the top is evident here. The correction function tends to make the simple plane waves less smooth, thus altering them in the direction required to produce atomic wave functions.

The energy of any state for the model crystal considered here depends on the binding parameter Za as follows:

$$aE/Z = f(Za).$$

Perturbation theory yields an expansion of the function $f(Za)$ for small values of the argument. The function $f(Za)$ is proportional to $(Za)^{-1}$ for small Za . The first three terms in this expansion were obtained in I for the four states considered. It is desirable to determine the region in which this expansion is reliable and, particularly in view of interest in systems with narrow d bands, to determine as much as possible about the energy bands in the limit of large Za . (Here we consider only the behavior of the energy bands, and do not investigate the question of the adequacy of the energy-band approximation itself.) Two methods are employed to study this problem.

It is possible to make considerable improvements with respect to perturbation theory by numerically diagonalizing a portion of the Hamiltonian matrix (using a basis of symmetrized linear combinations of plane waves). The results of this calculation are reported in Sec. IV for the four states pertaining to the body-centered cubic lattice studied in I. The results indicate that the three term expansion of perturbation theory gives reliable results up to $Za=25$. For larger values of

the binding parameter, perturbation theory gives an overestimate of the band width.

For large values of the binding parameter a tight-binding approximation is appropriate. This is discussed in Sec. V. It is found that the bandwidth must go to zero exponentially as the binding parameter increases. Crystal field effects in this model, however, decrease only as $(Za)^{-4}$ and thus ultimately dominate overlap effects for sufficiently large Za .⁴ Consequently, the d band must split into two sub-bands, one based (in the language of the tight binding approximation) on functions of xy , yz , and zx symmetries (t_{2g}) and the other on the e_g functions x^2-y^2 and $3z^2-r^2$. By comparing the crystal field splitting of the d levels with the bandwidth calculated on the basis of the tight-binding approximation, we obtain an estimate of $Za=70$ for the binding parameter at which this splitting first occurs.

A detailed calculation of d bands in a real crystal would have to include the effects of spin-orbit coupling. The effects of spin-orbit coupling on d band structure are studied in Sec. VI, in the tight-binding approximation. A general formulation of effective mass theory for d bands in the presence of spin-orbit coupling is also given.

II. THE FACE-CENTERED CUBIC LATTICE

The methods of I are immediately applicable to the face-centered cubic lattice. The Fourier coefficients of potential are (in atomic units):

$$\begin{aligned} V(\mathbf{k}) &= -8\pi Z/\Omega_0 k^2 = -8Z/\pi a n^2 \quad \text{for } \mathbf{k} \neq 0, \\ V(0) &= \pi Z/2a. \end{aligned} \quad (2-1)$$

In these equations $\Omega_0 = a^3/4$ is the volume of the unit cell and $\mathbf{k} = (2\pi/a)\mathbf{n}$ [where $\mathbf{n} = (n_1, n_2, n_3)$] is a reciprocal lattice vector.

The Brillouin zone for the face-centered cubic lattice is shown in Fig. 1. We consider here the two points of highest symmetry, Γ and X . At Γ , the irreducible representations of interest are Γ_{12} and $\Gamma_{25'}$, which are doubly degenerate and triply degenerate, respectively, (neglecting the spin degeneracy). At X , we are concerned with the representations X_2 , X_3 , and X_5 . The first two are not degenerate; X_5 is doubly degenerate. For the particular point $X = (2\pi/a)(1,0,0)$ (there are three inequivalent points X); X_2 transforms as $y^2 - z^2$; X_3 as yz , and X_5 as xy or xz . The representation X_1 , which is the completely symmetric one and thus includes s states, contains the d function whose symmetry is $2x^2 - y^2 - z^2$. Linear combinations of plane waves transforming according to all the representations of interest have been constructed according to the procedure described in the Appendix of a previous paper.⁵ From these, the matrix elements of the potential, which are linear combinations of the Fourier coefficients

⁴ J. Callaway and D. M. Edwards, Phys. Rev. 118, 923 (1960).

⁵ J. Callaway, Phys. Rev. 99, 500 (1955).

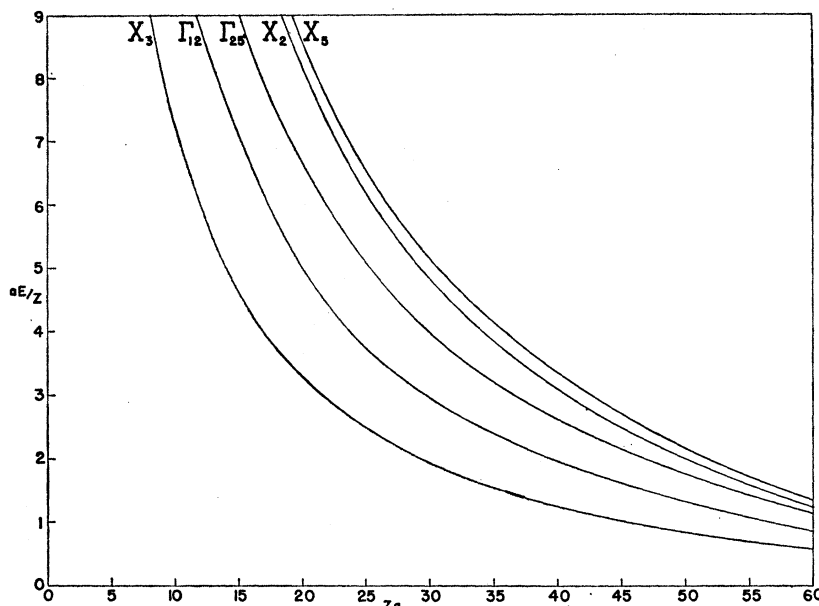


FIG. 2. The dimensionless quantity aE/Z is given as a function of Za for the five states considered.

(2-1) are easily obtained. The perturbation series carried to second order then yields the following results:

$$\begin{aligned}
 X_3: E &= 78.957/a^2 - 0.6159Z/a - 0.00319Z^2, \\
 \Gamma_{25'}: E &= 118.43/a^2 - 0.8281Z/a - 0.00484Z^2, \\
 \Gamma_{12}: E &= 157.91/a^2 - 1.0933Z/a - 0.00692Z^2, \\
 X_2: E &= 197.39/a^2 - 1.4329Z/a - 0.01057Z^2, \\
 X_5: E &= 197.39/a^2 - 0.9023Z/a - 0.01777Z^2.
 \end{aligned}
 \tag{2-2}$$

The results are shown in Fig. 2, where the dimensionless parameter aE/Z is plotted as a function of Za . The convergence of the expansions appears similar to that found in I for the body-centered cubic lattice. The order of levels given here (for small Za) is the same as that found for copper by Howarth in a cellular method calculation.⁶

Comparison of the energies of corresponding states pertaining to the body-centered and face-centered cubic lattices is interesting in that it illustrates the effect of the different boundary conditions on the wave functions. The comparison should be made in such a way that the volume of the atomic cell is the same in each case. The volume of the atomic cell in the body-centered lattice is $a_b^3/2$; in the face-centered lattice it is $a_f^3/4$. We now define a new "lattice parameter" a' such that $a'^3/2 = a_f^3/4$, where a_f is the ordinary lattice parameter for the face-centered cubic structure used in (2-1) and (2-2). When we express $a'E/Z$ as a function of Za' , the results may be compared directly with previous calculations for the body-centered cubic lattice. This is done in Fig. 3 for the states Γ_{12} and $\Gamma_{25'}$. It is seen that the states at the center of the zone are separated by a greater amount in the face-centered

lattice than in the body-centered lattice, for small values of the binding parameter. In the body-centered structure, these states are degenerate in an empty lattice.

The behavior of the energies of the states $\Gamma_{25'}$ and Γ_{12} for large values of Za as suggested by the perturbation series for the face-centered structure cannot be correct. It has been shown in previous work that $\Gamma_{25'}$ must lie below Γ_{12} at large Za .⁴ The separation there is due to the crystal field splitting mentioned previously. Consequently, use of only three terms of the complete perturbation series is certainly inadequate for $Za \geq 88$, the point at which crossover of these levels is predicted. We shall see later that the limit of usefulness of these series is more likely to be about $Za = 30$.

III. d ELECTRON WAVE FUNCTIONS

The perturbation technique employed for a calculation of the energies of states at symmetry points of the Brillouin zone may also be applied to determine the wave function at these points. The perturbation series for the wave function ψ_{m,k^i} (m th state belonging to the i th irreducible representation of wave vector \mathbf{k}) may be written as:

$$\psi_{m,k^i} = u_{m,k^i} + \sum_{s, s \neq m} \frac{V_{ms} u_{s,k^i}}{E_m^0(i, \mathbf{k}) - E_s^0(i, \mathbf{k})} \tag{3-1}$$

where the u_{s,k^i} are the wave functions for the unperturbed system. The (unperturbed) energies of these states are $E_s^0(i, \mathbf{k})$. In the following we shall suppress the labels i, \mathbf{k} , understanding that summations include only states belonging to the same irreducible representation. The V_{ms} are matrix elements of the crystal potential. There are no matrix elements connecting

⁶ D. J. Howarth, Proc. Roy. Soc. (London) **A220**, 513 (1953).

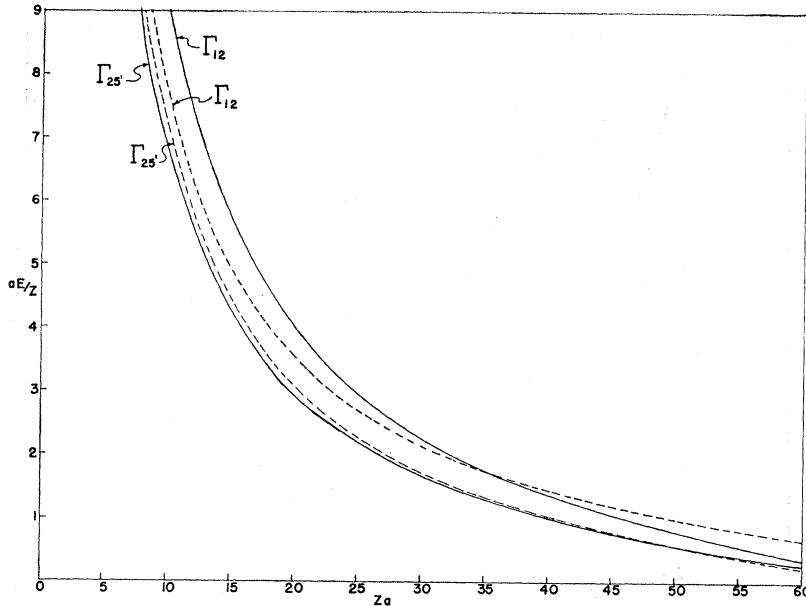


FIG. 3. Comparison of levels at the center of the zone for the face-centered cubic lattice (solid lines) and the body-centered cubic lattice (dotted lines).

different irreducible representations. These matrix elements are linear combinations of Fourier coefficients of the potential; consequently they are proportional to Z/a . The energy denominators are proportional to $1/a^2$ so that the first order perturbation term is proportional to the binding parameter Za . Each higher term includes an additional matrix element and an additional energy denominator, thus providing an additional power of Za . The perturbation series thus corrects the unperturbed function u_m by adding functions whose coefficients involve increasing powers of the binding parameter. These correction functions are expressed as Fourier series.

The basic functions u_s are symmetrized linear combinations of plane waves.⁷ In order to obtain a qualitative picture of the wave function, it is desirable to project out of the plane waves the spherical waves of principal interest: those with $l=2$. Of course, all spherical harmonics consistent with the cubic symmetry of ψ_m will be present in (3-1). Let $\Phi_m(r)$ be the $l=2$ component of ψ_m ; and χ_s the same component of u_s . These functions must contain the appropriate (normalized) Kubic harmonic, K_{2i} . Let

$$\Phi_m = F_m(r/a) K_{2i}(\theta, \phi), \quad (3-2)$$

and

$$\chi_m = f_m(r/a) K_{2i}(\theta, \phi).$$

The function $f_m(r/a)$ is proportional to a spherical

Bessel function. Since

$$u_m = \sum_{j=1}^N \frac{a_{m,j}}{\sqrt{N}} e^{i\mathbf{k}_m(j) \cdot \mathbf{r}}, \quad (3-3)$$

where the sum runs over an N -fold degenerate set of plane waves whose propagation vectors $\mathbf{k}_m(j)$ are reciprocal lattice vectors, and the coefficients $a_{m,j}$ are chosen to yield a wave function of the appropriate symmetry, the function f_m may be expressed as

$$f_m(r/a) = -4\pi \mathfrak{U}_m j_2(k_m r), \quad (3-4)$$

in which

$$\mathfrak{U}_m = \sum_j (a_{m,j}/\sqrt{N}) K_{2i}(\theta_j, \phi_j). \quad (3-5)$$

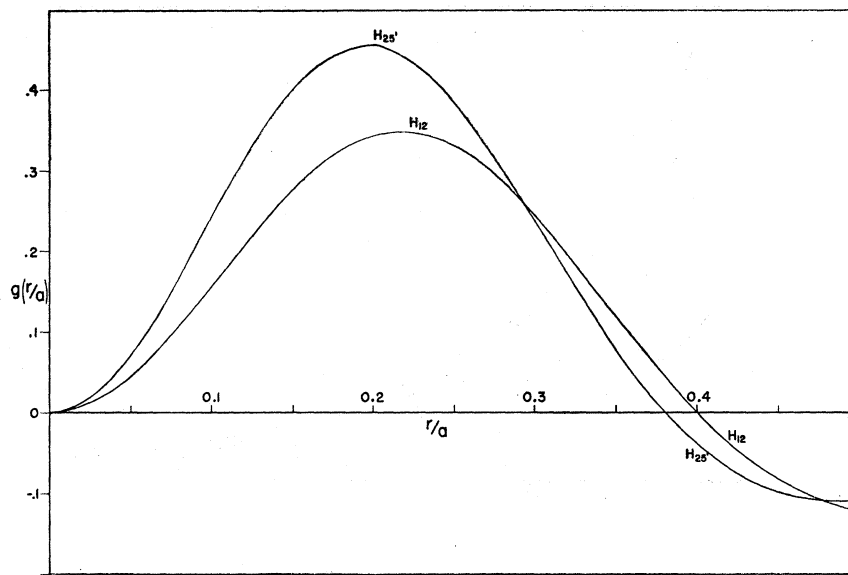
In these equations k_j , θ_j , ϕ_j are the spherical polar components of \mathbf{k}_j with respect to a fixed set of axes. It has been assumed here that the $a_{m,j}$ are of unit magnitude. This condition may not always be satisfied; but the resulting modification of (3-3) is trivial. We may now combine Eqs. (3-1) through (3-4) to obtain an expression for $F_m(r/a)$:

$$F_m(r/a) = -4\pi \left\{ \mathfrak{U}_m j_r(k_m r) + Za \sum_s \frac{(aV_{sm}/Z) \mathfrak{U}_s}{a^2(E_m^0 - E_s^0)} j_r(k_s r) \right\}. \quad (3-6)$$

Let the coefficient of Za in (3-6) be designated $g_m(r/a)$. This function has been evaluated numerically for the d electron states H_{12} and $H_{25'}$ pertaining to the body-centered cubic lattice. Since H_{12} is close to the bottom of the band and $H_{25'}$ is close to the top for small Za , we can obtain a qualitative idea of the variation of the wave function over the band from these two states.

⁷ A table of symmetrized linear combinations of plane waves for the body centered cubic lattice may be obtained from the author. This table has also been deposited as document No. 6391 with the ADI Auxiliary Publications Project, Photoduplication Service, Library of Congress, Washington 25, D. C. A copy may be secured by citing the Document number and by remitting \$1.25 for photoprints or \$1.25 for 35-mm microfilm. Advance payment is required. Make checks or money orders payable to Chief, Photoduplication Service, Library of Congress.

FIG. 4. First order correction function $g(r/a)$.



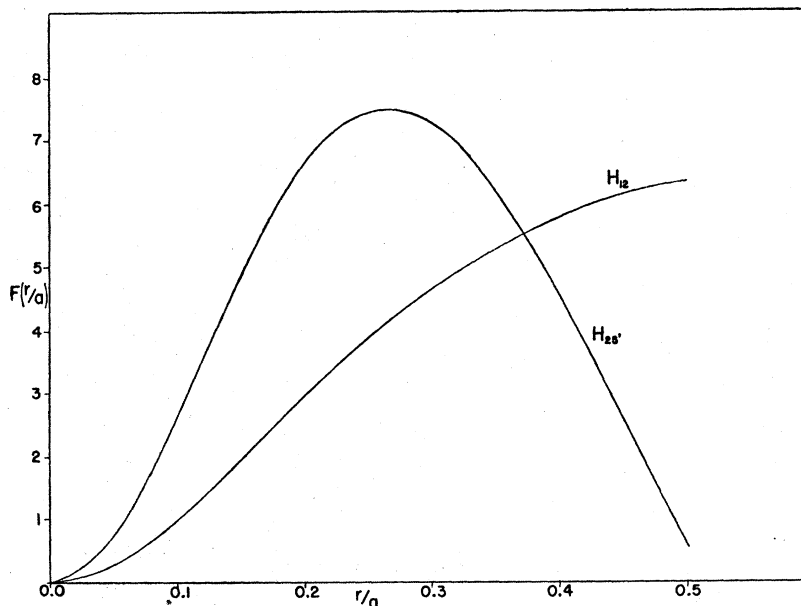
The computation included 102 plane waves for H_{12} and 144 for $H_{25'}$. The two functions $g_m(r/a)$ are shown in Fig. 4. In Fig. 5, the functions $F_m(r/a)$ are shown as obtained from (3-6) for $Za=20$.

Approximately 89% of the charge density for H_{12} and 80% of the charge density are in the $l=2$ angular momentum state for this Za . Corresponding values for the free electron functions are 87% and 68%, respectively.

The correction function has the expected property of reducing the amplitude of the wave function at large r and increasing it at small r , thus tending to produce wave functions of atomic character.

The wave functions of electrons in the d band of metallic iron have been studied recently by Wood³ and by Stern⁸ in order to determine whether the charge distribution of electrons in the metal might be more nearly uniform than in the free atom. These authors have emphasized that electrons at the bottom of the band have diffuse wave functions; those at the top have compact wave functions. The present calculation shows this property does not depend on the crystal potential and is characteristic even of wave functions in an empty lattice. It is interesting to see explicitly that the perturbation correction of the free electron wave functions, which tends to make them more nearly

FIG. 5. Radial part of $l=2$ component of the d state wave functions, normalized so that $\int \Omega_0 F^2(r) r^2 dr = 1$.



⁸ F. Stern, Bull. Am. Phys. Soc. 5, 169 (1960). Also see F. Stern, Phys. Rev. 116, 1399 (1959).

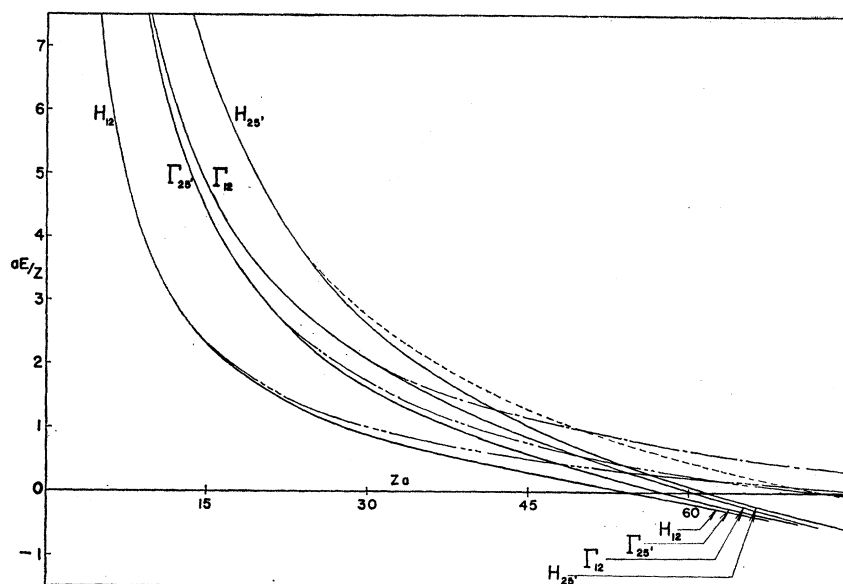


FIG. 6. Variation of aE/Z with Za for the four states in the body-centered cubic lattice according to sixth order plane wave expansions (solid lines) and perturbation theory (broken lines).

like atomic d functions, preserves this property of the free electron functions. Both of the functions presented here are, as expected, more diffuse than those obtained by Wood for metallic iron.

IV. INTERMEDIATE BINDING

As the binding parameter Za becomes large, the perturbation series expansion of the energy ceases to be useful. For an intermediate regime of values of the binding parameter, we may proceed as follows: We set up the matrix representation of the Hamiltonian according to the standard procedure still using plane waves for basis functions, and diagonalize a finite portion of it. The matrix elements of the potential are still linear combinations of Fourier coefficients of potential. By considering the dimensionless variable aE/Z , one can so arrange the matrix equation so that the off diagonal elements of H are constant, while the kinetic energy part of the diagonal elements contains $1/Za$. It is then not difficult to obtain numerically the energies of the states as functions of Za . This has been done for the four states Γ_{12} , $\Gamma_{25'}$, $H_{25'}$, and H_{12} pertaining to the body-centered cubic lattice which were considered in I. Sixth order matrices were considered in each case, thus including all plane waves through type $(2\pi/a)$ $(2,2,2)$ for Γ and $(2\pi/a)$ $(3,1,1)$ for H . The results are shown in Fig. 6, where they are compared with the perturbation solutions found in I.

Deviations from the results of perturbation theory begin to be seen around $Za=20$ or 25 . As expected, the energies of the states decrease more rapidly with increasing Za than is predicted by perturbation theory. The order of levels remains the same, however. For $Za>50$, perturbation theory predicts qualitatively incorrect results.

For values of the binding parameter for which this

procedure is adequate, the width of the d band is, approximately, the separation between $H_{25'}$ and H_{12} . This separation is shown in Fig. 7. It is evident that the bandwidth decreases in an essentially exponential manner for large Za . To a good approximation, we can write:

$$E(H_{25'}) - E(H_{12}) = (16Z/a)e^{-kZa}. \quad (4-1)$$

We find, approximately, $k=0.07$. It is probable, however, that this procedure yields an underestimate of the rate of decrease of the bandwidth.

V. TIGHT BINDING

As the binding is increased, the convergence of the plane wave expansion becomes poor since the kinetic energy terms in the diagonal matrix elements of the Hamiltonian become small. The tight-binding approximation is then appropriate. A simple form of the tight-binding method in which only two center integrals are included and the lack of orthogonality of the d functions on different atoms is neglected has been applied to the transition elements by Slater and Koster,⁹ and others.^{10,11}

If the interaction between electrons on nearest neighbor atoms alone is considered, the d -band structure in the body-centered cubic lattice is symmetric about its midpoint (in energy). When crystal field effects or second neighbor interactions are included, this symmetry is removed. We consider here principally the effect of including the nonspherical components of the crystal field.

The fourth-order multipole terms in the crystal

⁹ J. C. Slater and G. F. Koster, Phys. Rev. **94**, 1498 (1954).

¹⁰ G. C. Fletcher and E. P. Wohlfarth, Phil. Mag. **42**, 106 (1951); G. C. Fletcher, Proc. Phys. Soc. (London) **A65**, 192 (1952).

¹¹ M. Suffczynski, Acta. Phys. Polon. **15**, 287 (1956); **16**, 157, 161 (1957).

potential of a point charge lattice tend to lower the energies of states (in cubic lattices) whose wave functions are based on the Kubic harmonics xy, yz, zx (t_{2g} functions) with respect to those of symmetry $x^2 - y^2; 3z^2 - r^2$ (e_g functions). This effect is automatically included in the plane wave calculation described in the previous section; it may be included in a tight-binding calculation by adding a k -independent term ($6Dq$ in the conventional notation) to the diagonal matrix elements for functions of e_g symmetry and subtracting a term ($4Dq$) from the diagonal matrix elements of the t_{2g} functions.¹² There are no off diagonal elements of the crystal field. Effects due to bonding of the d orbitals, often discussed in the literature of crystal field theory are naturally included in the tight-binding calculation.

Qualitatively, it is easy to see that the crystal field tends to split the d band into two sub-bands based on the functions of e_g and t_{2g} symmetries, respectively. The effect is illustrated clearly in Fig. 8, in which the energy bands are shown along the $[100]$ axis in the Brillouin zone of the body-centered cubic lattice. The curves are obtained from a crude calculation using the results of Suffczynski¹¹ for interaction integrals. The calculation employs an unscreened Coulomb potential $2Z/r$ around each ion (for this reason energy values

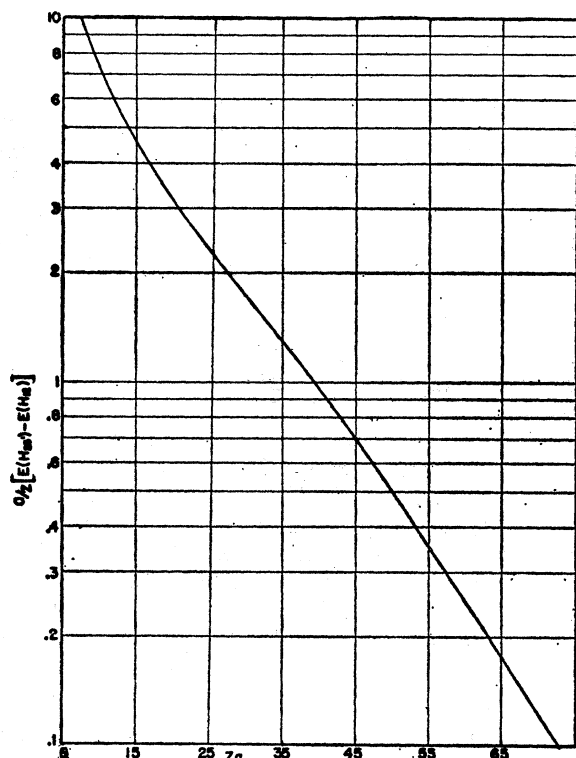


FIG. 7. Bandwidth (defined as the separation between $H_{25'}$ and H_{12}) as a function of Za from the plane wave expansions.

¹² A review of crystal field theory is given by W. Moffitt and C. J. Ballhausen, *Ann. Rev. Phys. Chem.* **7**, 107 (1956).

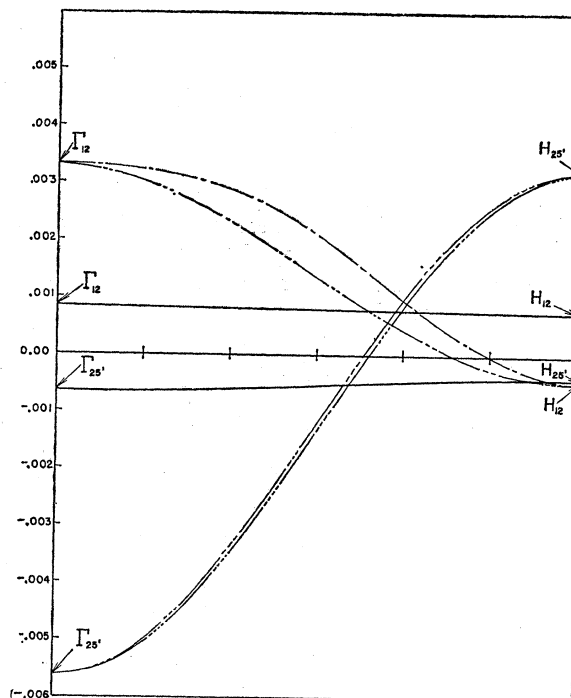


FIG. 8. Effect of crystal field splitting on d bands along the $[100]$ axis according to the tight-binding approximation. Broken lines correspond to $\beta=20$, solid lines to $\beta=25$.

cannot be compared directly with those of the previous section) and considers second neighbor interactions, but neglects the lack of orthogonality of wave functions on different atoms. Crystal field effects are included as described previously, numerical values being obtained from reference 4.

If we consider hydrogenic d state radial wave functions:

$$R_d = (\alpha^7/6!)^{1/2} r^2 e^{-\alpha r}, \quad (5-1)$$

and let R_1 be the nearest neighbor distance, the band quantities are functions of the variable

$$\beta = \frac{1}{2} \alpha R_1 = (\sqrt{3}/4) \alpha a. \quad (5-2)$$

The curves in Fig. 8 are drawn for $\beta=20$ and $\beta=25$, respectively ($\alpha a=46.2$ and 57.7 , respectively). The case $\beta=20$ is one in which the crystal field splitting $10Dq$ is about one half the bandwidth produced by the interaction integrals. In the case $\beta=25$, corresponding to the extreme tight-binding limit, the crystal field splitting is about eight times the bandwidth. For the present purposes, the bandwidth produced by the interaction integrals is defined as the separation between $H_{25'}$ and H_{12} in the absence of a crystal field splitting. From the work of Suffczynski¹¹ one has, considering first neighbors

$$(a/Z)[E(H_{25'}) - E(H_{12})] = 0.04562\beta^6(1+1/\beta)e^{-\beta}. \quad (5-3)$$

Several interesting qualitative results may be noted. First, the effect of the crystal field in separating the d

levels into two sub-bands is clearly seen. Similar results may be expected in other crystallographic directions, although some degeneracy present in this case will be removed. Second, it will be observed that the band formed from the t_{2g} functions is broader than that based on the e_g functions. This occurs because the width of the t_{2g} band is determined by the integral $(dd\sigma)_1$. (The notation used here is that of Slater and Koster for two center integrals⁸; however, here the subscripts 1 and 2 refer to nearest and second nearest neighbors in the body-centered cubic lattice.) The width of the e_g band is determined by $(dd\pi)_1$. Since $(dd\sigma)_1$ is proportional to $\beta^6 e^{-\beta}$ while $(dd\pi)_1$ is proportional to $\beta^5 e^{-\beta}$, the conclusion follows. Third, the splitting of the degeneracies of the bands along the 100 axis is accomplished by second neighbor interactions. The splitting of the e_g band is determined by the $(dd\sigma)_2$ integrals while that of the t_{2g} band depends on the $(dd\pi)_2$ integrals. Consequently, the e_g band is split to a greater extent. Also, the second neighbor integrals fall off exponentially as $\exp(-2\beta/\sqrt{3})$, so for large β , the splitting of the sub-bands falls off more rapidly than the bandwidth. The discussion in regard to point three applies, however, only to bands along the [100] axis. There is a first order interaction splitting of the sub-bands in other directions.

Finally, we wish to estimate the value of αa at which the crystal field splitting of the bands is equal to the overlap splitting. The crystal field effect is obtained from reference 4 as:

$$(\alpha/Z)10Dq = 1.492 \times 10^4 (\alpha a)^{-4}. \quad (5-4)$$

It is easily determined graphically that the overlap splitting given by (5-4) equals the crystal field splitting for $\alpha a = 48.5$. For values of αa greater than this, we may expect the d bands to be split into two sub-bands. As a rough approximation, we may set $\alpha = 2Z/3$, where Z is the ionic charge (this is the value for a pure Coulomb potential). If we consider $a = 6$ (iron has $a = 5.4$), then for the splitting to occur, we must have, approximately, $Z = 12$. It would seem to be unreasonable to expect a model involving completely separate d sub-bands to apply to iron, as has been proposed by Mott and Stevens¹³ and others.

The rough calculations of this section may be criticized in two respects: neglect of the lack of orthogonality of the wave functions on the different atoms, and the neglect of the screening of the Coulomb potential. A more accurate tight-binding calculation including these effects is being carried out by Mr. D. M. Edwards. The results will be reported at a later date.

VI. SPIN-ORBIT COUPLING

The consequences of including spin-orbit coupling in band theory have been discussed in a general way by Elliott, who has given character tables for some of the

double space groups of principal interest.¹⁴ The only application to d bands of which I am aware is that of Lehman, who has considered the $6d$ band of the actinide metals.¹⁵ He has considered, in what amounts to a tight-binding approximation, a face-centered cubic lattice with (effectively) a moderate value of the binding parameter and a relatively large spin-orbit coupling. The effects of spin-orbit coupling are also of interest in the case of narrow d bands. Our treatment here will concern principally body-centered cubic lattices, although much of the discussion will apply to any cubic structure.

The most striking effect of spin-orbit coupling is the removal of degeneracies. The $\Gamma_{25'}$ state, which is sixfold degenerate when spin is included is split into a doubly degenerate level Γ_7^+ lying above a fourfold degenerate level Γ_8 . If we write the spin-orbit coupling as a perturbation in the approximate form

$$V_s = \zeta \mathbf{L} \cdot \mathbf{S}, \quad (6-1)$$

the separation between these two states is $3\zeta/2$ provided ζ is small compared to the separation between the original $\Gamma_{25'}$ level and the Γ_{12} state. The latter, Γ_{12} , level is not split by the spin-orbit interaction. (It is however, raised in energy by an amount proportional to ζ^2 .) The splittings at H are similar to those at Γ .

There are two representations for states along the [100] axis: Δ_6 and Δ_7 . For this axis $\Gamma_7 \rightarrow \Delta_7$ and $\Gamma_8 \rightarrow \Delta_6 + \Delta_7$. The state Δ_5 fourfold degenerate in the absence of spin-orbit coupling is split into the doubly degenerate Δ_6 and Δ_7 . Since bands of the same symmetry do not cross, there is a profound modification of the band structure near the points of cross over. Since the 100 axis is now the only one with nontrivial symmetry properties, no accidental degeneracies or crossovers of bands will be permitted on other axes, and significant effects on the band structure must be expected.

To determine the form of the bands in detail, it is convenient to use the tight-binding approach. It is desirable to express the matrix representing the spin-orbit coupling on the basis of Kubic Harmonics. These functions (always assumed normalized) have the symmetry $xy, yz, xz, x^2 - y^2, 2z^2 - x^2 - y^2$, (numbered 1 through 5, respectively). They may be combined with spin functions for up and down (+ and -) spin. One first constructs the matrix of $\mathbf{L} \cdot \mathbf{S}$ on the basis of spherical harmonics according to the procedures given by Condon and Shortley¹⁶ and then transforms to the basis above. When this is done, the resulting 10×10 matrix may be factored by rearrangement of rows and columns into two essentially identical 5×5 matrices. On the basis of functions (in order): $x^2 - y^2(+)$, $2z^2 - x^2 - y^2(+)$, $ixy(+)$, $xz(-)$, $iyz(-)$, a 5×5 matrix

¹⁴ R. J. Elliott, Phys. Rev. **96**, 280 (1954).

¹⁵ Guy W. Lehman, Phys. Rev. **116**, 846 (1959).

¹⁶ E. U. Condon and G. H. Shortley, *Theory of Atomic Spectra* (Cambridge University Press, New York, 1935), p. 120.

¹³ N. F. Mott and K. W. H. Stevens, Phil. Mag. **2**, 1364 (1957).

is:

$$\zeta \begin{pmatrix} 0 & 0 & 1 & \frac{1}{2} & -\frac{1}{2} \\ 0 & 0 & 0 & \sqrt{3}/2 & \sqrt{3}/2 \\ 1 & 0 & 0 & -\frac{1}{2} & \frac{1}{2} \\ \frac{1}{2} & \sqrt{3}/2 & -\frac{1}{2} & 0 & -\frac{1}{2} \\ -\frac{1}{2} & \sqrt{3}/2 & \frac{1}{2} & -\frac{1}{2} & 0 \end{pmatrix}. \quad (6-2)$$

The matrix of the entire effective Hamiltonian may now be constructed. If, for example, H_{15} is the (real) tight binding matrix element connecting the functions

of symmetry xy and $2z^2-x^2-y^2$ (only functions of the same spin are connected in this way),¹⁷ then the Hamiltonian matrix can be put in the form:

$$H = \begin{pmatrix} M & N \\ N & M \end{pmatrix}, \quad (6-3)$$

in which M and N are the following 5×5 matrices (same basis as 6-2, extended by including functions of reversed spin)

$$M = \begin{pmatrix} H_{44} & H_{45} & \zeta + iH_{14} & \zeta/2 & -\zeta/2 \\ H_{45} & H_{55} & iH_{15} & \zeta\sqrt{3}/2 & \zeta\sqrt{3}/2 \\ -iH_{14} + \zeta & -iH_{15} & H_{11} & -\zeta/2 & \zeta/2 \\ \zeta/2 & \zeta\sqrt{3}/2 & -\zeta/2 & H_{33} & iH_{23} - \zeta/2 \\ -\zeta/2 & \zeta\sqrt{3}/2 & \zeta/2 & -iH_{23} - \zeta/2 & H_{22} \end{pmatrix}, \quad (6-4)$$

$$N = \begin{pmatrix} 0 & 0 & 0 & H_{43} & iH_{42} \\ 0 & 0 & 0 & H_{53} & iH_{52} \\ 0 & 0 & 0 & -iH_{13} & H_{12} \\ H_{43} & H_{53} & iH_{13} & 0 & 0 \\ -iH_{42} & -iH_{52} & H_{12} & 0 & 0 \end{pmatrix}.$$

The tight-binding matrix elements may be expanded in powers of k . If the integrals representing interactions between neighbors are regarded as parameters to be determined either from experiment or from a more rigorous theoretical calculation, we have a formulation equivalent to that called $\mathbf{k} \cdot \mathbf{p}$ perturbation theory by Kane.¹⁸ The only significant difference between this approach and that adopted by Kane for germanium, silicon, and indium antimonide is that we do not diagonalize the spin-orbit coupling initially since the separation between the states Γ_{12} and $\Gamma_{25'}$ will ordinarily be greater than the spin orbit splittings. Consequently, states of definite j, m_j are not particularly suitable basis functions.

The matrix elements may be written:

$$\begin{aligned} H_{11} &= d_t + A(k_x^2 + k_y^2) + Bk_z^2, \\ H_{12} &= Ck_x k_y, \\ H_{13} &= Ck_y k_z, \\ H_{14} &= 0, \\ H_{15} &= -2Dk_x k_y, \\ H_{22} &= d_i + A(k_y^2 + k_z^2) + Bk_x^2, \\ H_{23} &= Ck_x k_y, \\ H_{24} &= -\sqrt{3}Dk_y k_z, \\ H_{25} &= Dk_y k_z, \\ H_{33} &= d_t + A(k_x^2 + k_z^2) + Bk_y^2, \\ H_{34} &= \sqrt{3}Dk_y k_z, \\ H_{35} &= Dk_x k_z, \\ H_{44} &= d_e + E(k_x^2 + k_y^2) + Fk_z^2, \\ H_{45} &= G(k_x^2 - k_y^2), \\ H_{55} &= d_e + J(k_x^2 + k_y^2) + Kk_z^2. \end{aligned} \quad (6-5)$$

The quantities $d_t, d_e, A \dots K$ are the parameters in terms of which the bands are described. These expressions may be obtained either by expansion of the tight-binding matrix elements or directly from symmetry considerations. The following additional relations are also obtained:

$$\begin{aligned} E &= J - \frac{2}{3}\sqrt{3}G, \\ F &= J - \frac{1}{3}\sqrt{3}G, \\ K &= J - \sqrt{3}G. \end{aligned} \quad (6-6)$$

This discussion applies to any cubic crystal and could be used, for instance, to describe a d -band semiconductor with band extrema at $k=0$ if such exist.

For a general point in the Brillouin zone, it is necessary to diagonalize the full 10×10 Hamiltonian. For points along the $[001]$ axis, considerable simplification is possible, since all off diagonal matrix elements of the tight binding Hamiltonian are zero and $H_{22} = H_{33}$. The secular equation may then be factored into two identical quadratic and two identical cubic equations. The quadratic equation gives the energies of the levels of Δ_6 symmetry; the cubic, the Δ_7 levels.

The energies of the Δ_6 states are given by

$$2E = (H_{22} + H_{55} - \zeta/2) \pm (H_{55} - H_{22}) \times \left[1 + \frac{\zeta}{H_{55} - H_{22}} + \frac{25\zeta^2}{4(H_{55} - H_{22})^2} \right]^{\frac{1}{2}}. \quad (6-7)$$

The energies of the Δ_7 states are determined as the

¹⁷ These matrix elements may be obtained from the work of Slater and Koster (reference 9) provided allowance is made for crystal field effects in the manner described in Sec. V.

¹⁸ E. O. Kane, J. Phys. Chem. Solids **1**, 83 (1956); **1**, 249 (1956).

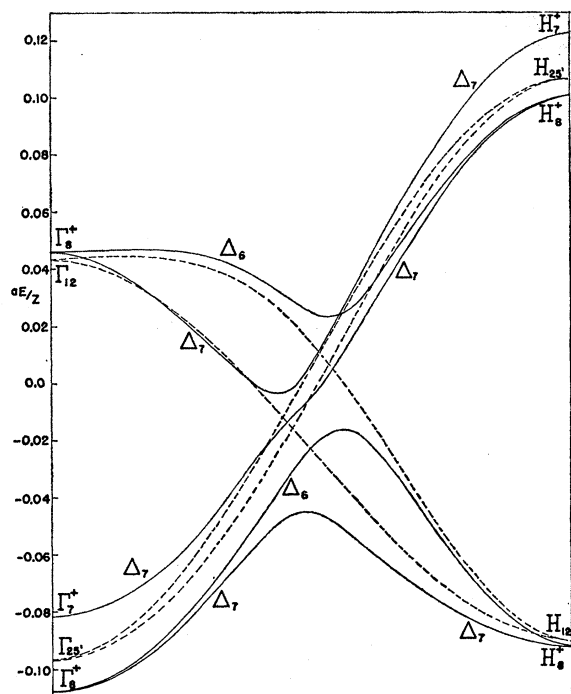


FIG. 9. Effect of spin-orbit coupling on d bands along the $[100]$ axis for $\beta=15$, $\alpha\zeta/Z=0.016$ (solid lines). Dotted lines are bands without inclusion of spin-orbit coupling.

roots of the equation (we put $E=H_{11}+\zeta-\lambda$):

$$\lambda^3 + (\gamma + \delta - 5\zeta/2)\lambda^2 + [\gamma(\delta - 3\zeta/2) - 2\delta\zeta]\lambda = \zeta\gamma\delta, \quad (6-8)$$

in which $\gamma=H_{44}-H_{11}$; $\delta=H_{22}-H_{11}$. The quantity δ vanishes at $k=0$, so that at this point a root (Γ_7^+), $E=H_{11}+\zeta$ is found. The remaining two different (Γ_7^+) roots at $k=0$, given by (6-7) and (6-8) agree since at that point $H_{44}=H_{55}$. These results agree with those of Lehman.¹⁴

Equations (6-7) and (6-8) have been applied to sketch the d bands along the 001 axis of the Brillouin zone of a body-centered cubic lattice. The tight binding

formulas of Sec. V were used. The evaluation was made for $\beta=15$, ($\alpha a=34.6$). A relatively large spin-orbit coupling $\alpha\zeta/Z=0.016$ was employed in order to emphasize for illustrative purposes the effect of the spin-orbit interaction. The results are shown in Fig. 9. The most important result of the spin-orbit coupling is the removal of several degeneracies: not only are the $\Gamma_{25'}$ and $H_{25'}$ levels split, but most of the accidental degeneracy along the axis is removed as well. There is only one crossover of Δ_6 and Δ_7 levels. A small increase in the bandwidth (if determined from these four states) can also be noticed. One observes that it might be possible to have some carriers of small effective mass present even when the overall d bandwidth is small.

By way of application to the actual transition metals, the effects of spin-orbit coupling on the band structure must be qualitatively similar to those encountered in this simple example. Of course, in the iron series, the spin-orbit coupling will not be as large compared to the bandwidth as that used here.

In the extreme tight-binding limit discussed in Sec. 5, in which crystal field effects have caused a splitting of the d bands into sub-bands based on functions of t_{2g} and e_g symmetries, the principal effect of spin-orbit coupling will be to split the lower, t_{2g} , band by an energy approximately $3\zeta/2$. (We have assumed $10Dq \gg \zeta$.) Except for this splitting, the form of the bands will be that shown in Fig. 8 for $\beta=25$.

ACKNOWLEDGMENTS

I am indebted to Mr. D. M. Edwards and to Dr. M. Suffczynski for discussions and correspondence on many aspects of the d band problem. The help of Mr. R. Abrines with respect to the material in Sec. II is gratefully acknowledged. This work was begun when the author was visiting professor in the Department of Mathematics, Queen Mary College, University of London. I also wish to thank Dr. R. A. Buckingham and the staff of the University of London computing center for their assistance with the calculations described in Sec. IV.